Passivity-Based Dynamic Visual Feedback Control for Three-Dimensional Target Tracking: Stability and L_2-Gain Performance Analysis

Masayuki Fujita, *Member, IEEE*, Hiroyuki Kawai, *Member, IEEE*, and Mark W. Spong, *Fellow, IEEE*

***Abstract*—This paper investigates vision-based robot control based on passivity for three-dimensional (3-D) target tracking. First, using standard body-attached coordinate frames (the world frame, camera frame, and object frame), we represent the relative position and orientation between a moving target and a camera as an element of $SE(3)$. Using this representation we derive a nonlinear observer to estimate the relative rigid body motion from the measured camera data. We then establish the relationship between the estimation error in a 3-D workspace and in the image plane. We show passivity of the dynamic visual feedback system by combining the passivity of both the visual feedback system and the manipulator dynamics which allows us to prove stability in the sense of Lyapunov for the full 3-D dynamic visual feedback system. The L_2-gain performance analysis, which deals with the disturbance attenuation problem, is then considered via dissipative systems theory. Finally, experimental results are presented to verify the stability and L_2-gain performance of the dynamic visual feedback system.**

***Index Terms*—L_2-gain performance analysis, Lyapunov stability, manipulator dynamics, passivity-based control, visual feedback control.**

I. Introduction

ROBOTICS and intelligent machines need sensory information to behave autonomously in dynamical environments. Visual information is particularly suited to recognize unknown surroundings. Vision-based control of robotic systems involves the fusion of robot kinematics, dynamics, and computer vision to control the motion of the robot in an efficient manner. The combination of mechanical control with visual information, so-called visual feedback control or visual servoing, is important when we consider a mechanical system working under dynamical environments [1], [2]. Recent applications of visual feedback control include the autonomous injection of biological cells [3], laparoscopic surgery [4], and others.

In classical visual servoing, many practical methods are reported with experimental results, e.g., see [5] and [6]. Specifically, several approaches that originate from classical visual servoing have been proposed to overcome the drawbacks that have been identified in experiments [7]. For the pose estimation problem, Lu *et al.* [8] derive an iterative algorithm which is globally convergent by using object space collinearity error. In [9], the 2 1/2-dimensional (2 1/2-D) visual servoing which incorporates the advantages of both position- and image-based visual servoing is proposed in order to guarantee robustness with respect to calibration errors. Partitioned visual servoing is considered in [10] in order to guarantee that all features remain in the image. More recently, an approach based on switching between position-based visual servoing and backward motion is investigated for dealing with the field-of-view problem [11]. However, classical visual servoing algorithms assume that the manipulator dynamics is negligible and does not interact with the visual feedback loop. This assumption, while it holds for kinematic control problems, is invalid for high-speed tasks.

Kelly [12] considered the set-point control problem with a static target for dynamic visual feedback system that includes the manipulator dynamics. Maruyama *et al.* [13] discussed robust control of the eye-in-hand system for the set-point control problem. For the moving target problem, Maruyama *et al.* used an adaptive H_∞ control approach based on passivity for a dynamic visual feedback system with parametric uncertainty [14]. In [15], Bishop *et al.* proposed an inverse dynamics-based control law for the problems of position tracking and the camera calibration in dynamic visual servoing. Recently, Zergeroglu *et al.* [16] developed an adaptive control law for position tracking and camera calibration in dynamic visual feedback control with parametric uncertainties. Although these control laws guarantee Lyapunov stability and are effective for the dynamic visual feedback system, they are restricted to planar manipulators.

For the problem of three-dimensional (3-D) visual servo control, Kelly *et al.* [17] considered an image-based controller under the assumption that the objects' depths are known. Cowan *et al.* [18] addressed the field-of-view problem for 3-D dynamic visual feedback system using navigation functions. Although good solutions to the set-point control problem are reported in those papers, few results have been obtained for the tracking problem of moving target objects in the full 3-D dynamic visual feedback system that include not only the position and the orientation but also the manipulator dynamics.

This paper deals with vision-based robot motion control for a moving target object in 3-D workspace with the eye-in-hand configuration as depicted in Fig. 1. Our proposed method is classified as position-based visual servoing, because we suggest the mapping from feature error in a image plane-to-rigid body

Manuscript received May 17, 2005; revised January 6, 2006. Manuscript received in final form July 10, 2006. Recommended by Associate Editor L. Villani.

M. Fujita is with the Department of Mechanical and Control Engineering, Tokyo Institute of Technology, Tokyo 152-8550, Japan (e-mail: fujita@ctrl.titech.ac.jp).

H. Kawai is with the Department of Robotics, Kanazawa Institute of Technology, Ishikawa 921-8501, Japan (e-mail: hiroyuki@neptune.kanazawa-it.ac.jp).

M. W. Spong is with the Coordinated Science Laboratory, University of Illinois at Urbana-Champaign, Urbana, IL 61801 USA (e-mail: mspong@uiuc.edu).

Color versions of Figs. 10–21 are available online at http://ieeexplore.ieee.org.

Digital Object Identifier 10.1109/TCST.2006.883236

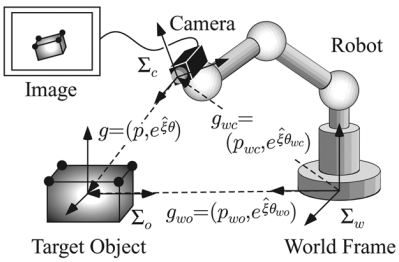

Fig. 1. Eye-in-hand visual feedback system.

error in a Cartesian space. This paper is organized as follows. In Section II, we derive a representation for relative rigid body motion using homogeneous representations and the adjoint transformations. In Section III, we present a nonlinear observer that estimates the relative rigid body motion from image data. The visual feedback system is constructed in Section IV and in Section V, based on our previous work in [19] and [20], we show passivity of the dynamic visual feedback system combined with the manipulator dynamics and present stability analysis. In Section VI, we present L_2-gain performance analysis via dissipative system theory. In Section VII, we present experiment results for dynamic visual feedback control on a 2-degrees-of-freedom (2-DOF) manipulator. Finally, we offer some conclusions in Section VIII.

II. Relative Rigid Body Motion in Visual Feedback System

A. Notation and Definition

Throughout this paper, we use the notation $e^{\hat{\xi}\theta_{ab}} \in \mathcal{R}^{3\times 3}$ to represent the rotation matrix of a frame Σ_b relative to a frame Σ_a. $\xi_{ab} \in \mathcal{R}^3$ specifies the direction of rotation and $\theta_{ab} \in \mathcal{R}$ is the angle of rotation. For simplicity, we use $\hat{\xi}\theta_{ab}$ to denote $\hat{\xi}_{ab}\theta_{ab}$. The notation "$\wedge$" (wedge) is the skew-symmetric operator such that $\hat{a}b = a \times b$ for the vector cross-product $\times$ and any vector $a, b \in \mathcal{R}^3$, i.e., $\hat{a}$ is a 3×3 skew-symmetric matrix. The vector space of all 3×3 skew-symmetric matrices is denoted $so(3)$. The notation "$\vee$" (vee) denotes the inverse operator to "$\wedge$," i.e., $so(3) \to \mathcal{R}^3$. Recall that a skew-symmetric matrix corresponds to an axis of rotation (via the mapping $a \mapsto \hat{a}$).

The transformation $e^{\hat{\xi}\theta_{ab}}$ is orthogonal with unit determinant and, hence, an element of the Lie group $SO(3) = \{e^{\hat{\xi}\theta_{ab}} \in \mathcal{R}^{3\times 3} \mid e^{\hat{\xi}\theta_{ab}}e^{-\hat{\xi}\theta_{ab}} = e^{-\hat{\xi}\theta_{ab}}e^{\hat{\xi}\theta_{ab}} = I_3, \det(e^{\hat{\xi}\theta_{ab}}) = +1\}$. The configuration space of the rigid body motion is the product space of $\mathcal{R}^3$ with $SO(3)$, which is denoted as $SE(3)$ throughout this paper (see, e.g., [21]). We use the 4×4 matrix

$$g_{ab} = \begin{bmatrix} e^{\hat{\xi}\theta_{ab}} & p_{ab} \\ 0 & 1 \end{bmatrix} \tag{1}$$

as the homogeneous representation of $g_{ab} = (p_{ab}, e^{\hat{\xi}\theta_{ab}}) \in SE(3)$ describing the configuration of a frame Σ_b relative to a frame Σ_a.

The adjoint transformation associated with g_{ab}, written $\mathrm{Ad}_{(g_{ab})}$, is given by

$$\mathrm{Ad}_{(g_{ab})} = \begin{bmatrix} e^{\hat{\xi}\theta_{ab}} & \hat{p}_{ab}e^{\hat{\xi}\theta_{ab}} \\ 0 & e^{\hat{\xi}\theta_{ab}} \end{bmatrix}. \tag{2}$$

Similar to the definition of $so(3)$, we define $se(3) := \{(v, \hat{\omega}) : v \in \mathcal{R}^3, \hat{\omega} \in so(3)\}$. In homogeneous representation, we write an element $\hat{V} \in se(3)$ as

$$\hat{V} = \begin{bmatrix} \hat{\omega} & v \\ 0 & 0 \end{bmatrix}. \tag{3}$$

An element of $se(3)$ is referred to as a twist. We call $V := (v, \omega)$ the twist coordinates of $\hat{V}$. If $\hat{V} \in se(3)$ is a twist with twist coordinates $V \in \mathcal{R}^6$, then for any $g \in SE(3)$, $g\hat{V}g^{-1}$ is a twist with twist coordinates $\mathrm{Ad}_{(g)}V \in \mathcal{R}^6$ ([21, Ch. 2, pp. 56, Lemma 2.13]). In other words, if $\hat{V}' = g\hat{V}g^{-1}$, then

$$V' = \mathrm{Ad}_{(g)}V \tag{4}$$

holds. This property concerning the adjoint transformation is important for the rigid body motion.

B. Basic Representation for Visual Feedback System

The visual feedback system considered in this paper, has the camera mounted on the robot's end-effector as depicted in Fig. 1, where the coordinate frames Σ_w, Σ_c, and Σ_o represent the world frame, the camera (end-effector) frame, and the object frame, respectively. Let $p_{co} \in \mathcal{R}^3$ and $e^{\hat{\xi}\theta_{co}} \in SO(3)$ be the position vector and the rotation matrix from the camera frame Σ_c to the object frame Σ_o. Then, the relative rigid body motion from Σ_c to Σ_o can be represented by $g_{co} = (p_{co}, e^{\hat{\xi}\theta_{co}}) \in SE(3)$. Similarities in $g_{\mathrm{wc}} = (p_{\mathrm{wc}}, e^{\hat{\xi}\theta_{\mathrm{wc}}})$ and $g_{\mathrm{wo}} = (p_{\mathrm{wo}}, e^{\hat{\xi}\theta_{\mathrm{wo}}})$ denote the rigid body motions from the world frame Σ_w to the camera frame Σ_c and from the world frame Σ_w to the object frame Σ_o, respectively, as shown in Fig. 1.

The objective of visual feedback control is to bring the actual relative rigid body motion $g_{co} = (p_{co}, e^{\hat{\xi}\theta_{co}})$ to a given reference $g_d = (p_d, e^{\hat{\xi}\theta_d})$. The reference g_d is assumed to be constant throughout this paper, because the camera can track the moving target object in this case.

We first derive a basic representation for the three coordinate frames of the visual feedback system. The relative rigid body motion involves the velocity of each rigid body. To this aim, let us consider the velocity of a rigid body as described in [21]. We define the body velocity of the camera relative to the world frame Σ_w as

$$\begin{aligned} \hat{V}^b_{\mathrm{wc}} &= g^{-1}_{\mathrm{wc}}\dot{g}_{\mathrm{wc}} = \begin{bmatrix} \hat{\omega}_{\mathrm{wc}} & v_{\mathrm{wc}} \\ 0 & 0 \end{bmatrix} \in \mathcal{R}^{4\times 4} \\ V^b_{\mathrm{wc}} &= \begin{bmatrix} v_{\mathrm{wc}} \\ \omega_{\mathrm{wc}} \end{bmatrix} \in \mathcal{R}^6 \end{aligned} \tag{5}$$

where v_{wc} and ω_{wc} represent the velocity of the origin and the angular velocity from Σ_w to Σ_c, respectively ([21 Ch. 2,

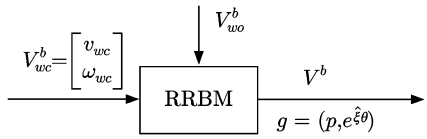

Fig. 2. Block diagram of the basic representation for the visual feedback system. RRBM is an acronym for Relative Rigid Body Motion in this figure.

(2.55)]). Similar to the body velocity of the target object relative to Σ_w will be denoted as

$$\hat{V}^b_{\rm wo} = g^{-1}_{\rm wo}\dot{g}_{\rm wo} = \begin{bmatrix} \hat{\omega}_{\rm wo} & v_{\rm wo} \\ 0 & 0 \end{bmatrix} \in \mathcal{R}^{4\times 4}$$
$$V^b_{\rm wo} = \begin{bmatrix} v_{\rm wo} \\ \omega_{\rm wo} \end{bmatrix} \in \mathcal{R}^6 \tag{6}$$

where $v_{\rm wo}$ and $\omega_{\rm wo}$ are the velocity of the origin and the angular velocity from Σ_w to Σ_o, respectively.

With $g = (p, e^{\hat{\xi}\theta})$ and V^b denoting $g_{co} = (p_{co}, e^{\hat{\xi}\theta_{co}})$ and V^b_{co} for short, respectively, the body velocity of the relative rigid body motion g can be written as

$$V^b = -{\rm Ad}_{(g^{-1})}V^b_{\rm wc} + V^b_{\rm wo}. \tag{7}$$

Equation (7) is a standard formula for the relation between the body velocities of three coordinate frames ([21 Ch. 2, pp. 59, Proposition 2.15]). We consider that it is the basic representation for the three coordinate frames of the visual feedback system. Fig. 2 shows the block diagram of this representation. Roughly speaking, the relative rigid body motion $g = (p, e^{\hat{\xi}\theta})$ will depend on the difference between the camera velocity $V^b_{\rm wc}$ and the target object velocity $V^b_{\rm wo}$, because V^b is defined as the body velocity of the relative rigid body motion g.

We next define the error vector of the rotation matrix $e^{\hat{\xi}\theta}$ as

$$e_R(e^{\hat{\xi}\theta}) := {\rm sk}(e^{\hat{\xi}\theta})^\vee \tag{8}$$

where ${\rm sk}(e^{\hat{\xi}\theta})$ denotes $(1/2)(e^{\hat{\xi}\theta} - e^{-\hat{\xi}\theta})$. Using this notation, we define $e_r := \left[p^T \; e^T_R(e^{\hat{\xi}\theta})\right]^T$. Then, we have the following lemma relating the body velocity of the camera $V^b_{\rm wc}$ to the vector form of the relative rigid body motion e_r.

Lemma 1: If the target object is static, i.e., $V^b_{\rm wo} = 0$, then the following inequality holds for the basic representation (7):

$$\int_0^T \left(V^b_{\rm wc}\right)^T(-e_r)dt \geq -\beta_r \tag{9}$$

where β_r is a positive scalar.

Proof: Consider the positive definite function

$$V_r = \frac{1}{2}||p||^2 + \phi(e^{\hat{\xi}\theta}) \tag{10}$$

where $\phi(e^{\hat{\xi}\theta}) := (1/2){\rm tr}(I - e^{\hat{\xi}\theta})$ is the error function of the rotation matrix and which has the following properties (see, e.g., [22]):

1) $\phi(e^{\hat{\xi}\theta}) = \phi(e^{-\hat{\xi}\theta}) \geq 0$ and $\phi(e^{\hat{\xi}\theta}) = 0$, if and only if $e^{\hat{\xi}\theta} = I_3$;
2) $\dot{\phi}(e^{\hat{\xi}\theta}) = e^T_R(e^{\hat{\xi}\theta})e^{\hat{\xi}\theta}\omega$.

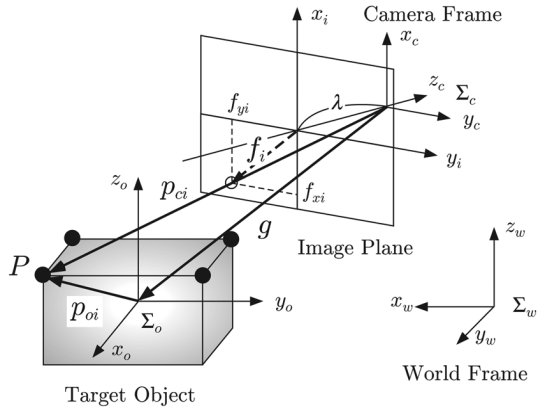

Fig. 3. Simple camera model.

Evaluating the time derivative of V_r along the trajectories of (7) gives us

$$\begin{aligned}\dot{V}_r &= p^T\dot{p} + e^T_R(e^{\hat{\xi}\theta})e^{\hat{\xi}\theta}\omega = p^T e^{\hat{\xi}\theta}e^{-\hat{\xi}\theta}\dot{p} + e^T_R(e^{\hat{\xi}\theta})e^{\hat{\xi}\theta}\omega \\ &= \begin{bmatrix} p^T & e^T_R(e^{\hat{\xi}\theta}) \end{bmatrix}\begin{bmatrix} e^{\hat{\xi}\theta} & 0 \\ 0 & e^{\hat{\xi}\theta} \end{bmatrix}\begin{bmatrix} v \\ \omega \end{bmatrix} \\ &= e^T_r {\rm Ad}_{(e^{\hat{\xi}\theta})}V^b = -e^T_r {\rm Ad}_{(e^{\hat{\xi}\theta})}{\rm Ad}_{(g^{-1})}V^b_{\rm wc} \\ &= -e^T_r\,{\rm Ad}_{(-p)}V^b_{\rm wc}\end{aligned} \tag{11}$$

where we use the definition of the body velocity ([21, Ch. 2, (2.55)]), i.e., $v = e^{-\hat{\xi}\theta}\dot{p}$. From the property of "$\wedge$" (wedge), we have $p^T\hat{p}\omega_{\rm wc} = -p^T\hat{\omega}_{\rm wc}p = 0$. Using this fact, we can obtain

$$\dot{V}_r = \left(V^b_{\rm wc}\right)^T(-e_r)\,. \tag{12}$$

Integrating (12) from 0 to T yields

$$\int_0^T \left(V^b_{\rm wc}\right)^T(-e_r)dt = V_r(T) - V_r(0) \geq -V_r(0) := -\beta_r \tag{13}$$

where β_r is the positive scalar which only depends on the initial state of $(p, e^{\hat{\xi}\theta})$. ■

Remark 1: Let us consider the body velocity of the camera $V^b_{\rm wc}$ as the input and the vector form of the relative rigid body motion $-e_r$ as its output. Then, Lemma 1 says that the basic representation for the visual feedback system (7) is *passive* from the input $V^b_{\rm wc}$ to the output $-e_r$ in the sense defined in [23].

C. Camera Model

The relative rigid body motion $g = (p, e^{\hat{\xi}\theta})$ cannot be immediately obtained in the visual feedback system because the target object velocity $V^b_{\rm wo}$ is unknown and, furthermore, cannot be measured directly. To control the relative rigid body motion using visual information provided by a computer vision system, we use the pinhole camera model with a perspective projection as shown in Fig. 3.

Let λ be a focal length, $p_{\rm oi} \in \mathcal{R}^3$ and $p_{\rm ci} \in \mathcal{R}^3$ be the position vectors of the target object's i-th feature point relative to Σ_o and Σ_c, respectively. Using a transformation of the coordinates, we have

$$p_{\rm ci} = gp_{\rm oi} \tag{14}$$

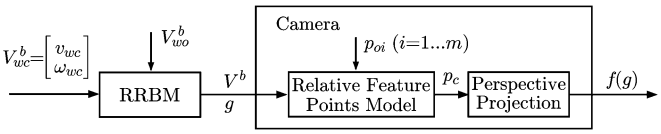

Fig. 4. Block diagram of the camera model with RRBM.

where $p_{\rm ci}$ and $p_{\rm oi}$ should be regarded, with a slight abuse of notation, as $\left[p_{\rm ci}^T\ 1\right]^T$ and $\left[p_{\rm oi}^T\ 1\right]^T$ via the well-known homogeneous coordinate representation in robotics, respectively (see, e.g., [21]).

The perspective projection of the ith feature point onto the image plane gives us the image plane coordinate $f_i := [f_{xi}\ f_{yi}]^T \in \mathcal{R}^2$ as

$$f_i = \frac{\lambda}{z_{\rm ci}} \begin{bmatrix} x_{\rm ci} \\ y_{\rm ci} \end{bmatrix} \tag{15}$$

where $p_{\rm ci} = [x_{\rm ci}\ y_{\rm ci}\ z_{\rm ci}]^T$. It is straightforward to extend this model to m image points by simply stacking the vectors of the image plane coordinate, i.e.,

$$f(g) := [\, f_1^T, \ldots, f_m^T \,]^T \in \mathcal{R}^{2m} \tag{16}$$

and $p_c := [\, p_{c1}^T \quad \ldots \quad p_{cm}^T \,]^T \in \mathcal{R}^{3m}$. We assume that multiple point features on a known object are given. Although the problem of extracting the feature points from the target object is interesting in its own right, we will not focus on this problem and merely assume that the feature points are obtained by well-known techniques. Under this assumption, the image information vector f depends only on the relative rigid body motion g from (14).

Fig. 4 shows the block diagram of the camera model with the relative rigid body motion as depicted in Fig. 2. The visual information $f(g)$ can be exploited, while the relative rigid body motion g cannot be obtained directly in the visual feedback system.

Remark 2: If the target object is static, then the passivity is preserved between the input as the part of the camera velocity $v_{\rm wc}$ and the output as the sum of the feature points relative to the camera frame $(-\sum_{i=1}^m p_{\rm ci})$ with the energy function $H := (1/2)\|p_c\|^2$, i.e., $\int_0^T \left(-\sum_{i=1}^m p_{\rm ci}\right)^T v_{\rm wc} \geq -\beta_H$, where β_H is a positive scalar. However, the system which includes the perspective projection does not preserve the passivity.

III. Nonlinear Observer and Estimation Error System

The visual feedback control task requires information of the relative rigid body motion g. Since the measurable information is only the image information in the visual feedback system, we consider a nonlinear observer in order to estimate the relative rigid body motion from the image information.

Using the basic representation (7), we choose estimates $\bar{g} = (\bar{p}, e^{\hat{\bar{\xi}}\bar{\theta}})$ and $\bar{V}^b$ of the relative rigid body motion and velocity, respectively, as

$$\bar{V}^b = -{\rm Ad}_{(\bar{g}^{-1})} V_{\rm wc}^b + u_e. \tag{17}$$

The new input $u_e = [\, v_{ue}^T \quad \omega_{ue}^T \,]^T$ is to be determined in order to drive the estimated values $\bar{g}$ and $\bar{V}^b$ to their actual values. The design of the input u_e is considered in Section IV.

Similarly to (14) and (15), the estimated image feature point $\bar{f}_i$ $(i = 1, \ldots, m)$ is defined as

$$\bar{p}_{\rm ci} = \bar{g} p_{\rm oi} \tag{18}$$

$$\bar{f}_i = \frac{\lambda}{\bar{z}_{\rm ci}} \begin{bmatrix} \bar{x}_{\rm ci} \\ \bar{y}_{\rm ci} \end{bmatrix} \tag{19}$$

where $\bar{p}_{\rm ci} := [\, \bar{x}_{\rm ci} \quad \bar{y}_{\rm ci} \quad \bar{z}_{\rm ci} \,]^T$. $\bar{f}(\bar{g}) := [\, \bar{f}_1^T, \ldots, \bar{f}_m^T \,]^T \in \mathcal{R}^{2m}$ means the m image points case.

In order to establish the estimation error system, we define the estimation error between the estimated value $\bar{g}$ and the actual relative rigid body motion g as

$$g_{\rm ee} = \bar{g}^{-1} g \tag{20}$$

in other words, $p_{\rm ee} = e^{-\hat{\bar{\xi}}\bar{\theta}}(p - \bar{p})$ and $e^{\hat{\xi}\theta_{\rm ee}} = e^{-\hat{\bar{\xi}}\bar{\theta}} e^{\hat{\xi}\theta}$. Note that $p = \bar{p}$ and $e^{\hat{\xi}\theta} = e^{-\hat{\bar{\xi}}\bar{\theta}}$ iff $g_{\rm ee} = I_4$, i.e., $p_{\rm ee} = 0$ and $e^{\hat{\xi}\theta_{\rm ee}} = I_3$. Using the notation $e_R(e^{\hat{\xi}\theta})$ defined in (8), the vector of the estimation error is given by

$$e_e := \left[\, p_{\rm ee}^T \quad e_R^T(e^{\hat{\xi}\theta_{\rm ee}}) \,\right]^T. \tag{21}$$

Note that $e_e = 0$ iff $p_{\rm ee} = 0$ and $e^{\hat{\xi}\theta_{\rm ee}} = I_3$. Therefore, if the vector of the estimation error is equal to zero, then the estimated relative rigid body motion $\bar{g}$ equals the actual relative rigid body motion g.

From the above, we derive a relation between the actual and estimated image information. Suppose the attitude estimation error $\theta_{\rm ee}$ is small enough that we can let $e^{\hat{\xi}\theta_{\rm ee}} \simeq I + {\rm sk}(e^{\hat{\xi}\theta_{\rm ee}})$. Then we have the following relation between the actual feature point $p_{\rm ci}$ and the estimated one $\bar{p}_{\rm ci}$

$$p_{\rm ci} - \bar{p}_{\rm ci} = e^{\hat{\bar{\xi}}\bar{\theta}} \left[\, I - \hat{p}_{\rm oi} \,\right] \begin{bmatrix} p_{\rm ee} \\ e_R(e^{\hat{\xi}\theta_{\rm ee}}) \end{bmatrix}. \tag{22}$$

Using a first-order Taylor expansion approximation, the relation between the actual image information and the estimated one can be expressed as

$$f_i - \bar{f}_i = \begin{bmatrix} \frac{\lambda}{\bar{z}_{\rm ci}} & 0 & -\frac{\lambda \bar{x}_{\rm ci}}{\bar{z}_{\rm ci}^2} \\ 0 & \frac{\lambda}{\bar{z}_{\rm ci}} & -\frac{\lambda \bar{y}_{\rm ci}}{\bar{z}_{\rm ci}^2} \end{bmatrix} (p_{\rm ci} - \bar{p}_{\rm ci}). \tag{23}$$

Let us define the image information error as $f_e := f(g) - \bar{f}(\bar{g})$. Hence, the relation between the actual image information and the estimated one can be given by

$$f_e = J(\bar{g}) e_e \tag{24}$$

where $J(\bar{g}) : SE(3) \to \mathcal{R}^{2m \times 6}$ is defined as

$$J(\bar{g}) := [\, J_1^T(\bar{g}) \quad J_2^T(\bar{g}) \quad , \ldots , \quad J_m^T(\bar{g}) \,]^T \tag{25}$$

$$J_i(\bar{g}) := \begin{bmatrix} \frac{\lambda}{\bar{z}_{\rm ci}} & 0 & -\frac{\lambda \bar{x}_{\rm ci}}{\bar{z}_{\rm ci}^2} \\ 0 & \frac{\lambda}{\bar{z}_{\rm ci}} & -\frac{\lambda \bar{y}_{\rm ci}}{\bar{z}_{\rm ci}^2} \end{bmatrix} \times e^{\hat{\bar{\xi}}\bar{\theta}} \left[\, I \quad -\hat{p}_{\rm oi} \,\right], \quad (i = 1, \ldots, m). \tag{26}$$

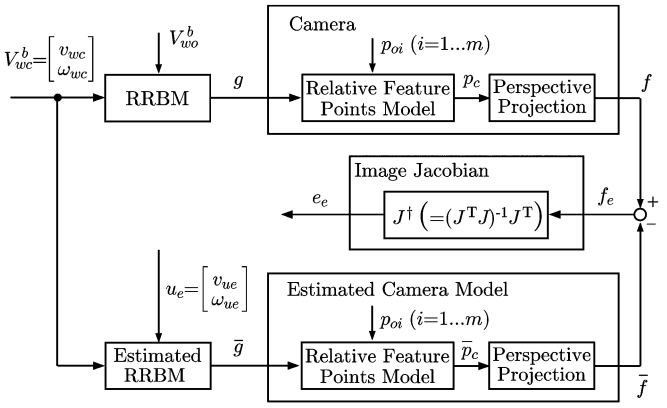

Fig. 5. Relation between the image information error f_e and the estimation error e_e.

Note that the matrix $J(\bar{g})$ represents the relationship between the estimation error in the 3-D workspace and in the image plane, while the well-known image Jacobian is the relationship between the velocity of the target object in the 3-D workspace and in the image plane [1]. We assume that the matrix $J(\bar{g})$ is full column rank for all $\bar{g} \in SE(3)$. Then, the relative rigid body motion can be uniquely defined by the image feature vector. Because this may not hold in some cases when $m = 3$, it is known that $m \geq 4$ is desirable for the full column rank of the image Jacobian [24].

The previous discussion shows that we can derive the vector of the estimation error e_e from image information f and the estimated value of the relative rigid body motion $(\bar{p}, e^{\hat{\bar{\xi}}\bar{\theta}})$

$$e_e = J^{\dagger}(\bar{g}) f_e \tag{27}$$

where † denotes the pseudo-inverse. Fig. 5 shows the relation between the image information error f_e and the estimation error e_e. Therefore, the estimation error e_e can be exploited in the 3-D visual feedback control law using image information f obtained from the camera. Hence, the nonlinear observer is constructed by (17)–(19) and the estimation input u_e, which can be determined from e_e in (27) with an estimation gain in Section IV.

The estimation error system will be derived in the same way as the basic representation for the visual feedback system. Differentiating (20) with respect to time and using (7) and (17), we obtain

$$V_{\rm ee}^b = -\mathrm{Ad}_{(g_{\rm ee}^{-1})} u_e + V_{\rm wo}^b. \tag{28}$$

Equation (28) represents the estimation error system.

Remark 3: Similar to the basic representation (7), if the target object is static, then the estimation error system (28) satisfies $\int_0^T u_e^T(-e_e)dt \geq -\beta_e$, where β_e is a positive scalar and, hence, preserves the passivity property of the basic representation.

IV. Visual Feedback System

A. Control Error System

Let us consider the dual of the estimation error system, which we call the control error system, in order to establish the visual feedback system. First, we define the control error as follows:

$$g_{\rm ec} = g_d^{-1} \bar{g} \tag{29}$$

which represents the error between the estimated value $\bar{g}$ and the reference of the relative rigid body motion g_d. It should be remarked that the estimated relative rigid body motion equals the reference one if and only if the control error is equal to the identity matrix in matrix form, i.e., $p_d = \bar{p}$ and $e^{\hat{\xi}\theta_d} = e^{\hat{\bar{\xi}}\bar{\theta}}$ iff $g_{\rm ec} = I_4$. Using the notation $e_R(e^{\hat{\xi}\theta})$, the vector of the control error is defined as

$$e_c := \left[p_{\rm ec}^T \quad e_R^T(e^{\hat{\xi}\theta_{\rm ec}}) \right]^T. \tag{30}$$

Note that $e_c = 0$ iff $p_{\rm ec} = 0$ and $e^{\hat{\xi}\theta_{\rm ec}} = I_3$. The vector of the control error can be made by the reference of the relative rigid body motion g_d and the estimated one $\bar{g}$ directly, while the vector of the estimation error must be obtained from the image information.

The reference of the relative rigid body motion g_d is assumed to be constant in this paper, i.e., $\dot{g}_d = 0$ and, hence, $V_{\rm ec}^b = \bar{V}^b$. Thus, the control error system can be represented as

$$\begin{aligned} V_{\rm ec}^b &= -\mathrm{Ad}_{(\bar{g}^{-1})} V_{\rm wc}^b + u_e \\ &= -\mathrm{Ad}_{(g_{\rm ec}^{-1})} \mathrm{Ad}_{(g_d^{-1})} V_{\rm wc}^b + u_e. \end{aligned} \tag{31}$$

This is dual to the estimation error system. Similar to the estimation error system, the control error system also preserves the passivity property of the basic representation.

B. Passivity of Visual Feedback System

Combining (28) and (31), we construct the visual feedback system as follows:

$$\begin{bmatrix} V_{\rm ec}^b \\ V_{\rm ee}^b \end{bmatrix} = \begin{bmatrix} -\mathrm{Ad}_{(g_{\rm ec}^{-1})} & I \\ 0 & -\mathrm{Ad}_{(g_{\rm ee}^{-1})} \end{bmatrix} u_{\rm ce} + \begin{bmatrix} 0 \\ I \end{bmatrix} V_{\rm wo}^b \tag{32}$$

where

$$u_{\rm ce} := \left[\left(\mathrm{Ad}_{(g_d^{-1})} V_{\rm wc}^b \right)^T \quad u_e^T \right]^T \tag{33}$$

denotes the control input. For the design of the visual feedback system, it is assumed that the camera velocity $V_{\rm wc}^b$ can be directly chosen. Let us define the error vector of the visual feedback system as

$$e := [\, e_c^T \quad e_e^T \,]^T \tag{34}$$

which consists of the control error vector e_c and the estimation error vector e_e. It should be noted that if the vectors of the control error and the estimation error are equal to zero, then the actual rigid body motion g, the estimated relative rigid body motion $\bar{g}$, and the reference motion g_d coincide. Therefore, the actual relative rigid body motion g tends to the reference one g_d when $e \to 0$.

Next, we show an important relation between the input and the output of the visual feedback system.

Lemma 2: If $V_{\rm wo}^b = 0$, then the visual feedback system (32) satisfies

$$\int_0^T u_{\rm ce}^T \nu_{\rm ce} dt \geq -\beta_{\rm ce} \qquad \forall\, T > 0 \tag{35}$$

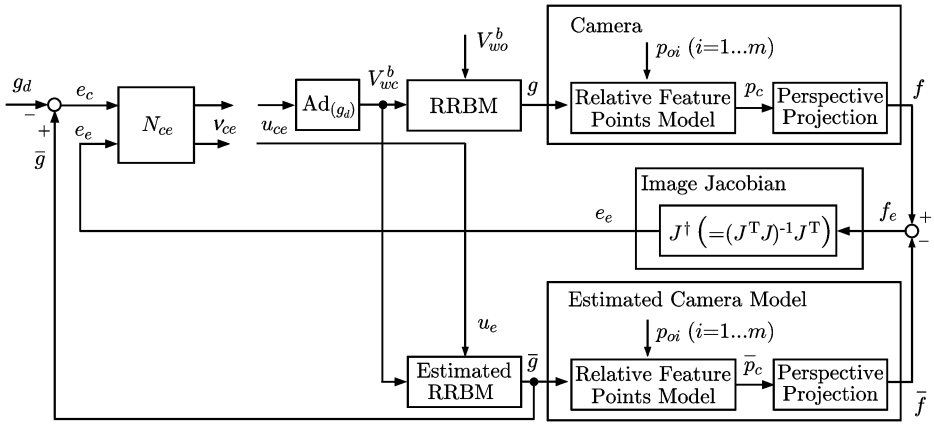

Fig. 6. Block diagram of the passivity of the visual feedback system. In this figure, the node performing between $\bar{g}$ and g_d gives only a conceptual meaning, since the difference between $\bar{g}$ and g_d is defined as $g_{\mathrm{ec}} = g_d^{-1}\bar{g} \in SE(3)$ and e_c is the vector form of g_{ec} as defined in (30).

where ν_{ce} is defined as

$$\nu_{\mathrm{ce}} := N_{\mathrm{ce}} e, \qquad N_{\mathrm{ce}} := \begin{bmatrix} -I & 0 \\ \mathrm{Ad}_{(e^{-\hat{\xi}\theta_{\mathrm{ec}}})} & -I \end{bmatrix} \tag{36}$$

and β_{ce} is a positive scalar.

Proof: Consider the following positive definite function:

$$V_{\mathrm{ce}} = \frac{1}{2}\|p_{\mathrm{ec}}\|^2 + \phi(e^{\hat{\xi}\theta_{\mathrm{ec}}}) + \frac{1}{2}\|p_{\mathrm{ee}}\|^2 + \phi(e^{\hat{\xi}\theta_{\mathrm{ee}}}). \tag{37}$$

The positive definiteness of the function V_{ce} results from the property of the error function ϕ. Differentiating (37) with respect to time yields

$$\begin{aligned} \dot{V}_{\mathrm{ce}} =& p_{\mathrm{ec}}^T e^{\hat{\xi}\theta_{\mathrm{ec}}} e^{-\hat{\xi}\theta_{\mathrm{ec}}} \dot{p}_{\mathrm{ec}} + e_R^T(e^{\hat{\xi}\theta_{\mathrm{ec}}}) e^{\hat{\xi}\theta_{\mathrm{ec}}} \omega_{\mathrm{ec}} \\ &+ p_{\mathrm{ee}}^T e^{\hat{\xi}\theta_{\mathrm{ee}}} e^{-\hat{\xi}\theta_{\mathrm{ee}}} \dot{p}_{\mathrm{ee}} + e_R^T(e^{\hat{\xi}\theta_{\mathrm{ee}}}) e^{\hat{\xi}\theta_{\mathrm{ee}}} \omega_{\mathrm{ee}} \\ =& \begin{bmatrix} p_{\mathrm{ec}}^T & e_R^T(e^{\hat{\xi}\theta_{\mathrm{ec}}}) & p_{\mathrm{ee}}^T & e_R^T(e^{\hat{\xi}\theta_{\mathrm{ee}}}) \end{bmatrix} \\ &\times \begin{bmatrix} \mathrm{Ad}_{(e^{\hat{\xi}\theta_{\mathrm{ec}}})} & 0 \\ 0 & \mathrm{Ad}_{(e^{\hat{\xi}\theta_{\mathrm{ee}}})} \end{bmatrix} \begin{bmatrix} V_{\mathrm{ec}}^b \\ V_{\mathrm{ee}}^b \end{bmatrix}. \end{aligned} \tag{38}$$

Using the skew-symmetry of the matrices $\hat{p}_{\mathrm{ec}}$ and $\hat{p}_{\mathrm{ee}}$, i.e.,

$$p_{\mathrm{ec}}^T \hat{p}_{\mathrm{ec}} \omega_{\mathrm{wc}} = -p_{\mathrm{ec}}^T \hat{\omega}_{\mathrm{wc}} p_{\mathrm{ec}} = 0$$

and

$$p_{\mathrm{ee}}^T \hat{p}_{\mathrm{ee}} \omega_{\mathrm{wc}} = -p_{\mathrm{ee}}^T \hat{\omega}_{\mathrm{wc}} p_{\mathrm{ee}} = 0$$

and substituting (32) into (38) yields

$$\begin{aligned} \dot{V}_{\mathrm{ce}} =& e^T \begin{bmatrix} \mathrm{Ad}_{(e^{\hat{\xi}\theta_{\mathrm{ec}}})} & 0 \\ 0 & \mathrm{Ad}_{(e^{\hat{\xi}\theta_{\mathrm{ee}}})} \end{bmatrix} \times \begin{bmatrix} -\mathrm{Ad}_{(g_{\mathrm{ec}}^{-1})} & I \\ 0 & -\mathrm{Ad}_{(g_{\mathrm{ee}}^{-1})} \end{bmatrix} u_{\mathrm{ce}} \\ =& e^T \begin{bmatrix} -\mathrm{Ad}_{(-p_{\mathrm{ec}})} & \mathrm{Ad}_{(e^{\hat{\xi}\theta_{\mathrm{ec}}})} \\ 0 & -\mathrm{Ad}_{(-p_{\mathrm{ee}})} \end{bmatrix} u_{\mathrm{ce}} \\ =& e^T \begin{bmatrix} -I & \mathrm{Ad}_{(e^{\hat{\xi}\theta_{\mathrm{ec}}})} \\ 0 & -I \end{bmatrix} u_{\mathrm{ce}} = u_{\mathrm{ce}}^T \nu_{\mathrm{ce}}. \end{aligned} \tag{39}$$

Integrating (39) from 0 to T, we obtain

$$\int_0^T u_{\mathrm{ce}}^T \nu_{\mathrm{ce}} dt = V_{\mathrm{ce}}(T) - V_{\mathrm{ce}}(0) \geq -V_{\mathrm{ce}}(0) := -\beta_{\mathrm{ce}} \tag{40}$$

where β_{ce} is the positive scalar which only depends on the initial states of $g_{\mathrm{ec}} = (p_{\mathrm{ec}}, e^{\hat{\xi}\theta_{\mathrm{ec}}})$ and $g_{\mathrm{ee}} = (p_{\mathrm{ee}}, e^{\hat{\xi}\theta_{\mathrm{ee}}})$. ■

The block diagram of the passivity of the visual feedback system is shown in Fig. 6.

Remark 4: Let us take u_{ce} as the input and ν_{ce} as its output in Fig. 6. Thus, Lemma 2 implies that the visual feedback system (32) is *passive* from the input u_{ce} to the output ν_{ce} as in the definition in [23]. It should be noted that this property is triggered by the relation of the basic representation for the visual feedback system (7) in Section II-B.

C. Visual Feedback Control and Stability Analysis

Based on the above passivity property of the visual feedback system, we consider the following control law:

$$u_{\mathrm{ce}} = -K_{\mathrm{ce}} N_{\mathrm{ce}} e, \qquad K_{\mathrm{ce}} := \begin{bmatrix} K_c & 0 \\ 0 & K_e \end{bmatrix} \tag{41}$$

where $K_c := \mathrm{diag}\{k_{c1}, \ldots, k_{c6}\}$ and $K_e := \mathrm{diag}\{k_{e1}, \ldots, k_{e6}\}$ are the positive gain matrices of x, y, and z axes of the translation and the rotation for the control error and the estimation error, respectively.

Theorem 1: If $V_{\mathrm{wo}}^b = 0$, then the equilibrium point $e = 0$ for the closed-loop system (32) and (41) is asymptotic stable.

Proof: In the proof of Lemma 2, we have already shown that the time derivative of V_{ce} along the trajectory of the system (32) is formulated as (39). Using the control input (41), (39) can be transformed into

$$\dot{V}_{\mathrm{ce}} = -e^T N_{\mathrm{ce}}^T K_{\mathrm{ce}} N_{\mathrm{ce}} e. \tag{42}$$

This completes the proof. ■

Theorem 1 shows Lyapunov stability for the visual feedback system. If the camera velocity is decided directly, the control objective is achieved by using the proposed control law (41).

V. Passivity-Based Dynamic Visual Feedback Control

A. Passivity of Dynamic Visual Feedback System

The dynamics of n-link rigid robot manipulators can be written as

$$M(q)\ddot{q} + C(q,\dot{q})\dot{q} + g(q) = \tau + \tau_d \tag{43}$$

where q, $\dot{q}$, and $\ddot{q}$ are the joint angle, velocity, and acceleration, respectively, τ is the vector of the input torque, and τ_d represents a disturbance input. $M(q) \in \mathcal{R}^{n\times n}$ is the manipulator inertia matrix, $C(q,\dot{q}) \in \mathcal{R}^{n\times n}$ is the Coriolis matrix and $g(q) \in \mathcal{R}^n$ is the gravity vector [25]. Equation (43) possesses several important properties which will be used in the sequel. The manipulator dynamics (43) is passive from τ to $\dot{q}$, that is $\int_0^T \tau^T \dot{q} dt \geq -\beta_m$, where β_m is a positive scalar. Moreover, $\dot{M}(q) - 2C(q,\dot{q})$ is skew-symmetric by defining $C(q,\dot{q})$ using the Christoffel symbols. The visual feedback system (32) and the manipulator dynamics (43) will be connected by the passivity. This is the reason why we discussed with the persistence of the passivity as mentioned in Remarks 1–4.

Now, we will construct a dynamic visual feedback system by connecting the visual feedback system (32) and the manipulator dynamics (43). First, we focus on the body velocity of the camera $V_{\rm wc}^b$, because it is concerned with the input of the visual feedback system and the output of the manipulator dynamics. Since the camera is mounted on the end-effector of the manipulator in the eye-in-hand configuration, the body velocity of the camera $V_{\rm wc}^b$ is given by

$$V_{\rm wc}^b = J_b(q)\dot{q} \tag{44}$$

where $J_b(q)$ is the manipulator Jacobian [21].

Next, we propose the control law for the manipulator as

$$\begin{aligned}\tau &= M(q)\ddot{q}_d + C(q,\dot{q})\dot{q}_d + g(q) + J_b^T(q)\mathrm{Ad}^T_{(g_d^{-1})}e_c + u_r \\ &= Y(q,\dot{q},\dot{q}_d,\ddot{q}_d)\psi + J_b^T(q)\mathrm{Ad}^T_{(g_d^{-1})}e_c + u_r \end{aligned} \tag{45}$$

where $\dot{q}_d$ and $\ddot{q}_d$ represent the desired joint velocity and acceleration, respectively. Y is a matrix of known functions and ψ is a constant vector of inertia parameters. The first term in (45) is the compensation of the nonlinear effects. The new input u_r is to be determined in order to achieve the control objective. Our control law is based on the motion controller which is proposed by Paden and Panja [26]. Although the desired joint angle and velocity could be given in the motion control, they will not be decided directly in the dynamic visual feedback system because of the unknown motion of the target object. Thus, our control law can not include the same position error $e_q := q - q_d$ as their control law includes. Hence, we consider the novel feedback term $J_b^T(q)\mathrm{Ad}^T_{(g_d^{-1})}e_c$ which includes the control error e_c via the transposed Jacobian approach in Cartesian space [12], [27].

We define the error vector with respect to the joint velocity of the manipulator dynamics as

$$r := \dot{q} - \dot{q}_d. \tag{46}$$

From the above discussion, we obtain the following error dynamics:

$$M(q)\dot{r} + C(q,\dot{q})r - J_b^T(q)\mathrm{Ad}^T_{(g_d^{-1})}e_c = u_r + \tau_d. \tag{47}$$

Remark 5: It is well known that the manipulator dynamics, (43) is passive from τ to $\dot{q}$ with $\tau_d = 0$. Also, the error dynamics is passive from the new input u_r to the error of the joint velocity r with $\tau_d = 0$, if we assume $e_c = 0$.

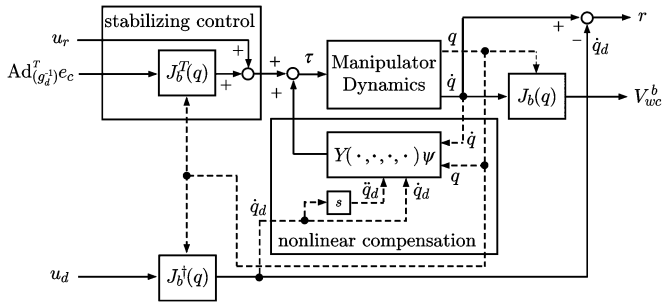

Fig. 7. Block diagram of the manipulator dynamics and the auxiliary controller with the desired camera velocity.

Moreover, we design the reference of the joint velocity based on the relation between the camera velocity and the joint velocity (44) as

$$\dot{q}_d := J_b^\dagger(q)u_d \tag{48}$$

where $u_d = [v_{ud}^T \quad \omega_{ud}^T]^T$ is the desired body velocity of the camera which will be obtained from the visual feedback system. The reference of the joint acceleration $\ddot{q}_d := -J_b^\dagger \dot{J}_b J_b^\dagger u_d + J_b^\dagger \dot{u}_d$ can be calculated, because u_d will be proposed as $\mathrm{Ad}_{(g_d)}K_c e_c$ afterward, and $\dot{u}_d$ can be obtained by K_c, g_d, $\bar{g}$, and $\dot{\bar{g}}$. The block diagram of the manipulator dynamics and the auxiliary controller with the desired camera velocity is depicted in Fig. 7. If the velocity error r is equal to zero, then the body velocity of the camera $V_{\rm wc}^b$ achieves the desired one u_d.

Using (32) and (47), the visual feedback system with manipulator dynamics (we call the dynamic visual feedback system) can be derived as follows:

$$\begin{aligned}\begin{bmatrix}\dot{r}\\ V_{\rm ec}^b\\ V_{\rm ee}^b\end{bmatrix} &= \begin{bmatrix}-M(q)^{-1}C(q,\dot{q})r + M(q)^{-1}J_b^T(q)\mathrm{Ad}^T_{(g_d^{-1})}e_c\\ -\mathrm{Ad}_{(\bar{g}^{-1})}J_b(q)r\\ 0\end{bmatrix} \\ &+ \begin{bmatrix}M(q)^{-1} & 0 & 0\\ 0 & -\mathrm{Ad}_{(g_{\rm ec}^{-1})} & I\\ 0 & 0 & -\mathrm{Ad}_{(g_{\rm ee}^{-1})}\end{bmatrix}u \\ &+ \begin{bmatrix}M(q)^{-1} & 0\\ 0 & 0\\ 0 & I\end{bmatrix}w \end{aligned} \tag{49}$$

where $u := [u_r^T \quad (\mathrm{Ad}_{(g_d^{-1})}u_d)^T \quad u_e^T]^T$. We define the state and the disturbance of dynamic visual feedback system as $x := [r^T \quad e_c^T \quad e_e^T]^T$ and $w := [\tau_d^T \quad (V_{\rm wo}^b)^T]^T$, respectively.

Before constructing the dynamic visual feedback control law, we derive an important lemma.

Lemma 3: If $w = 0$, then the dynamic visual feedback system (49) satisfies

$$\int_0^T u^T \nu dt \geq -\beta \qquad \forall\, T > 0 \tag{50}$$

where

$$\nu := Nx, \qquad N := \begin{bmatrix}I & 0 & 0\\ 0 & -I & 0\\ 0 & \mathrm{Ad}_{(e^{-\hat{\xi}\theta_{\rm ec}})} & -I\end{bmatrix} \tag{51}$$

and β is a positive scalar.

Proof: Consider the following positive definite function:

$$V = \frac{1}{2} r^T M(q) r + \frac{1}{2}\|p_{\rm ec}\|^2 + \phi(e^{\hat{\xi}\theta_{\rm ec}}) + \frac{1}{2}\|p_{\rm ee}\|^2 + \phi(e^{\hat{\xi}\theta_{\rm ee}}). \tag{52}$$

Differentiating (52) with respect to time yields

$$\begin{aligned}\dot{V} =& r^T M(q)\dot{r} + \frac{1}{2} r^T \dot{M}(q) r + p_{\rm ec}^T e^{\hat{\xi}\theta_{\rm ec}} e^{-\hat{\xi}\theta_{\rm ec}} \dot{p}_{\rm ec} \\ &+ e_R^T(e^{\hat{\xi}\theta_{\rm ec}}) e^{\hat{\xi}\theta_{\rm ec}} \omega_{\rm ec} + p_{\rm ee}^T e^{\hat{\xi}\theta_{\rm ee}} e^{-\hat{\xi}\theta_{\rm ee}} \dot{p}_{\rm ee} \\ &+ e_R^T(e^{\hat{\xi}\theta_{\rm ee}}) e^{\hat{\xi}\theta_{\rm ee}} \omega_{\rm ee} \\ =& x^T \begin{bmatrix} M(q) & 0 & 0 \\ 0 & {\rm Ad}_{(e^{\hat{\xi}\theta_{\rm ec}})} & 0 \\ 0 & 0 & {\rm Ad}_{(e^{\hat{\xi}\theta_{\rm ee}})} \end{bmatrix} \begin{bmatrix} \dot{r} \\ V_{\rm ec}^b \\ V_{\rm ee}^b \end{bmatrix} \\ &+ \frac{1}{2} r^T \dot{M}(q) r. \end{aligned} \tag{53}$$

Observing that the skew-symmetry of the matrices $\hat{p}_{\rm ec}$ and $\hat{p}_{\rm ee}$, i.e.,

$$p_{\rm ec}^T \hat{p}_{\rm ec} e^{-\hat{\xi}\theta_d}\omega_{ud} = -p_{\rm ec}^T (e^{-\hat{\xi}\theta_d}\omega_{ud})^\wedge p_{\rm ec} = 0$$
$$p_{\rm ee}^T \hat{p}_{\rm ee}\omega_{ue} = -p_{\rm ee}^T \hat{\omega}_{ue} p_{\rm ee} = 0$$

the previous equation along the trajectories of the system (49), can be transformed into

$$\begin{aligned}\dot{V} =& -r^T C(q,\dot{q}) r + r^T J_b^T(q) {\rm Ad}^T_{(g_d^{-1})} e_c \\ &- e_c^T {\rm Ad}_{(e^{\hat{\xi}\theta_{\rm ec}})} {\rm Ad}_{(\bar{g}^{-1})} J_b(q) r + \frac{1}{2} r^T \dot{M}(q) r \\ &+ x^T \begin{bmatrix} M(q) & 0 & 0 \\ 0 & {\rm Ad}_{(e^{\hat{\xi}\theta_{\rm ec}})} & 0 \\ 0 & 0 & {\rm Ad}_{(e^{\hat{\xi}\theta_{\rm ee}})} \end{bmatrix} \\ &\times \begin{bmatrix} M(q)^{-1} & 0 & 0 \\ 0 & -{\rm Ad}_{(g_{\rm ec}^{-1})} & I \\ 0 & 0 & -{\rm Ad}_{(g_{\rm ee}^{-1})} \end{bmatrix} u \\ =& \frac{1}{2} r^T (\dot{M} - 2C) r + r^T J_b^T(q) {\rm Ad}^T_{(g_d^{-1})} e_c \\ &- e_c^T {\rm Ad}_{(g_d^{-1})} J_b(q) r + x^T \begin{bmatrix} I & 0 & 0 \\ 0 & -I & {\rm Ad}_{(e^{\hat{\xi}\theta_{\rm ec}})} \\ 0 & 0 & -I \end{bmatrix} u \\ =& x^T N^T u. \end{aligned} \tag{54}$$

Integrating (54) from 0 to T, we obtain

$$\int_0^T u^T \nu dt = V(T) - V(0) \geq -V(0) := -\beta \tag{55}$$

where β is a positive scalar that only depends on the initial states of r, $g_{\rm ec}$, and $g_{\rm ee}$. ∎

Remark 6: The visual feedback system (32) satisfies the passivity property as described in (35). It is well known that the manipulator dynamics (43) also has the passivity. These passivity properties are connected by the manipulator Jacobian (44). In Lemma 3, the inequality (50) says that the dynamic visual feedback system (49) is *passive* from the input $u = \begin{bmatrix} u_r^T & ({\rm Ad}_{(g_d^{-1})} u_d)^T & u_e^T \end{bmatrix}^T$ to the output $\nu = \begin{bmatrix} r^T & \nu_{\rm ce}^T \end{bmatrix}^T$.

B. Dynamic Visual Feedback Control and Stability Analysis

We now propose the following control input for the interconnected system:

$$u = -K\nu = -KNx, \qquad K := \begin{bmatrix} K_r & 0 & 0 \\ 0 & K_c & 0 \\ 0 & 0 & K_e \end{bmatrix} \tag{56}$$

where $K_r := {\rm diag}\{k_{r1}, \ldots, k_{rn}\}$ denotes the positive gain matrix for each joint axis.

Theorem 2: If $w = 0$, then the equilibrium point $x = 0$ for the closed-loop system (49) and (56) is asymptotic stable.

Proof: In the proof of Lemma 3, we have already derived that the time derivative of V along the trajectory of the system (49) is formulated as (54). Using the control input (56) and (54) can be transformed into

$$\dot{V} = -x^T N^T K N x. \tag{57}$$

This completes the proof. ∎

Considering the manipulator dynamics, Theorem 2 shows the stability via Lyapunov method for the full 3-D dynamic visual feedback system. It is interesting to note that stability analysis is based on the passivity as described in (50). The block diagram of the dynamic visual feedback control is shown in Fig. 8. As depicted in Fig. 8, the block diagram of the dynamic visual feedback system consists of a parallel connection of the visual feedback system in Fig. 6 and the manipulator dynamics with the auxiliary controller in Fig. 7 with the body velocity $V_{\rm wc}^b$.

Because our proposed approach is based on the passivity, other passivity-based motion control laws, e.g., the adaptive motion control [28], the robust control [29], the velocity observer approach [26], and so on, can be applied to the dynamic visual feedback system by straight forward extensions.

VI. L_2-Gain Performance Analysis

In this section, we utilize L_2-gain performance analysis to evaluate the tracking performance of the control scheme in the presence of a moving target. The motion of the target object is regarded as an external disturbance. Hence, our approach is closely related to the so-called *disturbance attenuation problem* [30]–[32].

In order to derive a simple and practical gain condition, we redefine $K_e = k_e I$, where k_e is a positive scalar.

Theorem 3: Given a positive scalar γ, assume

$$k_e - \frac{1}{2\gamma^2} - \frac{1}{2} > 0 \tag{58}$$

$$K_c - \frac{1}{2} I - k_e \left(\frac{1+\gamma^2}{\gamma^2(2k_e - 1) - 1} \right) I > 0 \tag{59}$$

$$K_r - \frac{1}{2\gamma^2} I - \frac{1}{2} I > 0. \tag{60}$$

Then the closed-loop system (49) and (56) has L_2-gain $\leq \gamma$.

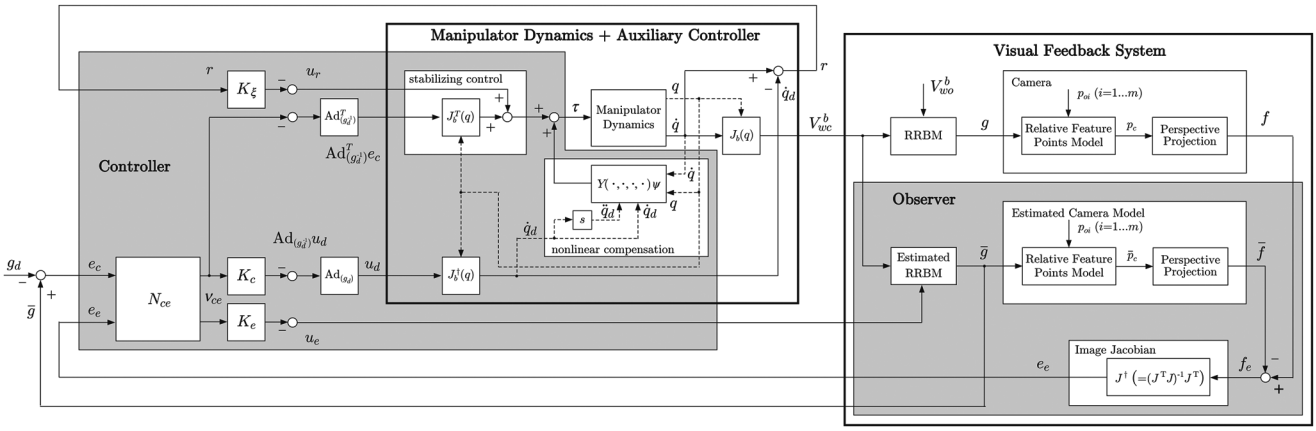

Fig. 8. Block diagram of the dynamic visual feedback control.

Proof: Differentiating the positive definite function V defined in (52) along the trajectory of the closed-loop system yields

$$\dot{V} = \frac{\gamma^2}{2}\|w\|^2 - \frac{1}{2}\|x\|^2 - \frac{\gamma^2}{2}\|w\|^2 + \frac{1}{2}\|x\|^2 + x^T \begin{bmatrix} I & 0 & 0 \\ 0 & -I & \mathrm{Ad}_{(e^{\hat{\xi}\theta_{\mathrm{ec}}})} \\ 0 & 0 & -I \end{bmatrix} u + x^T \begin{bmatrix} I & 0 \\ 0 & 0 \\ 0 & \mathrm{Ad}_{(e^{\hat{\xi}\theta_{\mathrm{ee}}})} \end{bmatrix} w. \tag{61}$$

By completing the squares, we have

$$\begin{aligned} &\dot{V} + \frac{1}{2}\|x\|^2 - \frac{\gamma^2}{2}\|w\|^2 \\ &\quad = -\frac{\gamma^2}{2}\left\| w - \frac{1}{\gamma^2}\begin{bmatrix} I & 0 & 0 \\ 0 & 0 & \mathrm{Ad}_{(e^{-\hat{\xi}\theta_{\mathrm{ee}}})} \end{bmatrix} x \right\|^2 \\ &\qquad + \frac{1}{2\gamma^2}\left\| \begin{bmatrix} I & 0 & 0 \\ 0 & 0 & \mathrm{Ad}_{(e^{-\hat{\xi}\theta_{\mathrm{ee}}})} \end{bmatrix} x \right\|^2 + x^T N^T u + \frac{1}{2}\|x\|^2 \\ &\quad \le \frac{1}{2\gamma^2} W \|x\|^2 + x^T N^T u + \frac{1}{2}\|x\|^2 \end{aligned} \tag{62}$$

where $W := \mathrm{diag}\{I, 0, I\}$. Substituting the control input (56) into (62), we obtain

$$\dot{V} + \frac{1}{2}\|x\|^2 - \frac{\gamma^2}{2}\|w\|^2 \le -x^T N^T K N x + \frac{1}{2\gamma^2} W \|x\|^2 + \frac{1}{2}\|x\|^2. \tag{63}$$

It can be verified that the inequality

$$\dot{V} + \frac{1}{2}\|x\|^2 - \frac{\gamma^2}{2}\|w\|^2 \le -x^T P x \le 0 \tag{64}$$

holds if $P := N^T K N - (1/2\gamma^2)W - (1/2)I$ is positive semi-definite. Integrating (64) from 0 to T and noticing $V(T) \ge 0$, we have

$$\int_0^T \|x\|^2 dt \le \gamma^2 \int_0^T \|w\|^2 dt + 2V(0) \qquad \forall\, T > 0. \tag{65}$$

From the Schur complement [33]

$$P = \left[\begin{array}{cc|c} K_r - \frac{1}{2\gamma^2}I - \frac{1}{2}I & 0 & 0 \\ 0 & K_c + k_e I - \frac{1}{2}I & -k_e \mathrm{Ad}_{(e^{\hat{\xi}\theta_{\mathrm{ec}}})} \\ \hline 0 & -k_e \mathrm{Ad}_{(e^{-\hat{\xi}\theta_{\mathrm{ec}}})} & \left(k_e - \frac{1}{2\gamma^2} - \frac{1}{2}\right)I \end{array}\right]. \tag{66}$$

can be modified as the conditions (58)–(60) in Theorem 3. ■

Remark 7: The conditions (58)–(60) can be regarded as an extension of the ones for the disturbance attenuation of the robot motion control which are described in Proposition 3.1 [31], although these are only sufficient conditions.

In this framework, γ can be considered as an indicator of the tracking performance. Although we have discussed L_2-gain performance analysis for a simple case, which deals with the disturbance attenuation problem, the proposed strategy can be extended for the other types of generalized plants of the dynamic visual feedback systems, e.g., an H_∞ optimization problem with L_2-gain from the external disturbance w to the controlled output $z := W \begin{bmatrix} x \\ u \end{bmatrix}$ (W is an appropriate weight matrix), similarly to the robot motion control.

VII. Experimental Case Study

The manipulator used in the experiments (see Fig. 9), is controlled by a digital signal processor (DSP) from dSPACE Inc., which utilizes a power PC 750 running at 480 MHz. Control programs are written in MATLAB and SIMULINK, and implemented on the DSP using the Real-Time Workshop and dSPACE Software which includes ControlDesk, Real-Time Interface, and so on. A PULNiX TM-7EX camera was attached at the tip of the manipulator. The video signals are acquired by a frame grabber board PicPort-Stereo-H4D and an image processing software HALCON. The sampling time of the controller and the frame rate provided by the camera are 1 ms and 30 ft/s, respectively. Hence, the image information f is renewed every 33 ms. The control law τ is interpolated every 1 ms using the most recent available data from the vision system. The difference between the sampling rate of the robot control and

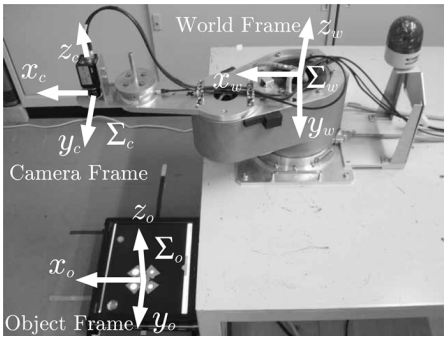

Fig. 9. Experimental setup with 2-DOF manipulator.

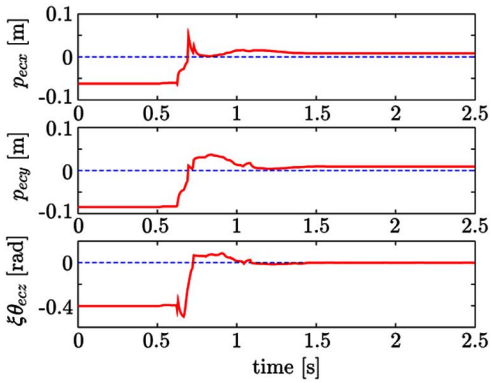

Fig. 10. Control error in the case of the static target object.

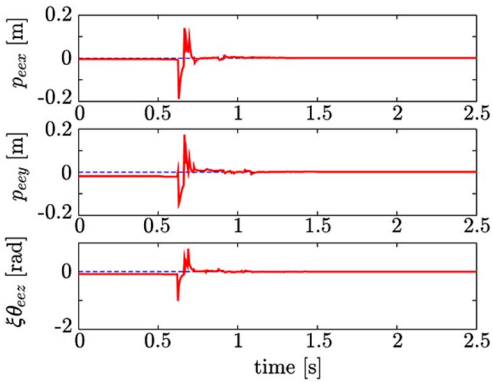

Fig. 11. Estimation error in the case of the static target object.

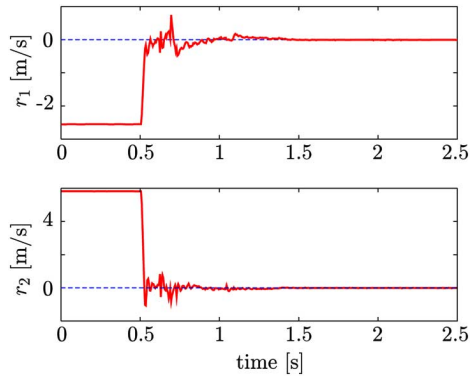

Fig. 12. Velocity error in the case of the static target object.

of the image grabbing can be decreased by using commercially available cameras with superior performance. The experimental results on 2-DOF manipulator as depicted in Fig. 9, are shown in order to understand our proposed method simply, though it is valid for 3-D dynamic visual feedback systems.

We define the three coordinate frames as in Fig. 9. The target object has four feature points that are projected onto the image plane of the camera. The target is a virtual object, programmed by using Virtual Reality Modeling Language (VRML) Toolbox with Matlab and displayed on a liquid crystal display. In this way, the position and orientation of the object are precisely known and, although these data are not needed in the control implementation, they can be used for subsequent analysis of the stability and L_2-gain performance of our controller.

A. *Stability Analysis in Experiment*

In this section, we present results for the stability analysis with a static target object. The experiment is carried out with the initial condition $q_1(0) = \pi/6$ rad, $q_2(0) = -\pi/6$ rad, $p_{\rm wo} = [0.4\ 0\ -0.81]^T$ m, $\xi\theta_{\rm wo} = [0\ 0\ -\pi/6]^T$ rad, $p_{\rm wc} = [0.4732\ 0.1\ 0]^T$ m, $\xi\theta_{\rm wc} = [0\ 0\ 0]^T$ rad. The desired relative rigid body motion $g_d = (p_d, e^{\hat{\xi}\theta_d})$ is $p_d = [0\ 0\ -0.81]^T$ m, $\xi\theta_d = [0\ 0\ 0]^T$ rad in these experiments.

The controller parameters for (56) were empirically selected as $K_r = \mathrm{diag}\{10, 10\}$, $K_c = \mathrm{diag}\{45, 45, 20, 20, 20, 40\}$, and $K_e = 40I_6$. The experimental results are shown in Figs. 10–13. Note that the torque input is added to the manipulator after 0.5 s for the safety measures which include the initialization of the image processing. Figs. 10–12 illustrate the control error e_c, the estimation error e_e, and the velocity error r, respectively. In Figs. 10 and 11, we focus on the errors of the translations of x and y and the rotation of z, because the errors of the translation of z and the rotations of x and y are zeros ideally on the defined coordinates in Fig. 9. The norm of the state x is shown in Fig. 13. From these figures, the asymptotic stability can be also confirmed experimentally.

B. *L_2-Gain Performance Analysis in Experiment*

Next, we present experimental results for the L_2-gain performance analysis in the case of a moving target object. In particular, we consider the disturbance attenuation problem by regarding the target motion as the disturbance for the dynamic visual feedback system. The target object moves along a straight line ($0 \le t < 4$) and a "Figure 8" motion ($4 \le t < 9.6$) as depicted in Fig. 14. The circle means the start point of the target object in these figures.

Here, we show a design procedure in order to assign the gains for the disturbance attenuation problem of the dynamic visual feedback system in the following.

Step 1) The control gain K_c is suitably selected.

Step 2) The estimation gain k_e satisfying the conditions (58) and (59) is decided.

Step 3) The velocity gain K_r satisfying the condition (60) is chosen for a given γ.

Based on the design procedure, the following gains were selected in order to confirm the adequacy of the L_2-gain performance for the dynamic visual feedback system in the following:

Gain A) $\gamma = 0.383$, $K_c = \mathrm{diag}\{10, 10, 5, 5, 5, 10\}$, $k_e = 30$, $K_r = \mathrm{diag}\{5, 5\}$;

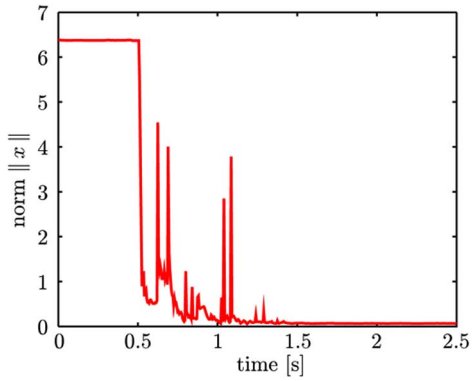

Fig. 13. Norm of the state in the case of the static target object.

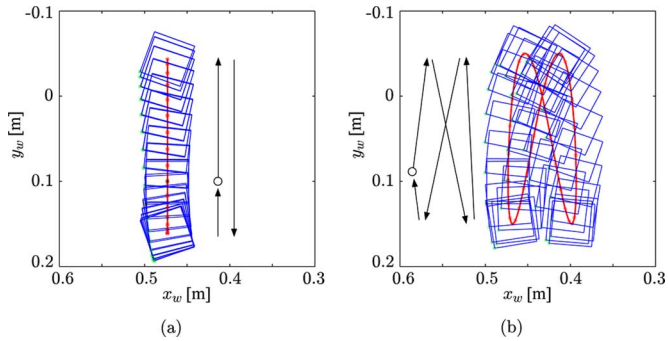

Fig. 14. Trajectory of the target object. (a) Straight line. (b) Figure 8 motion.

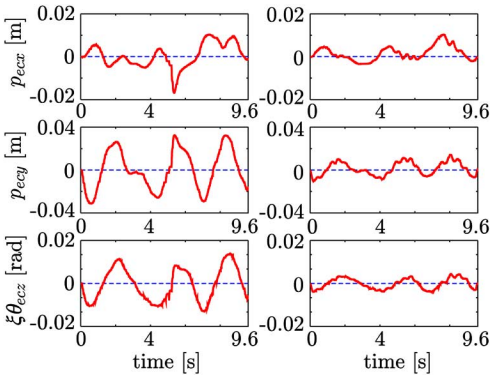

Fig. 15. Control error in the target tracking: left side: with Gain A; right side: with Gain B.

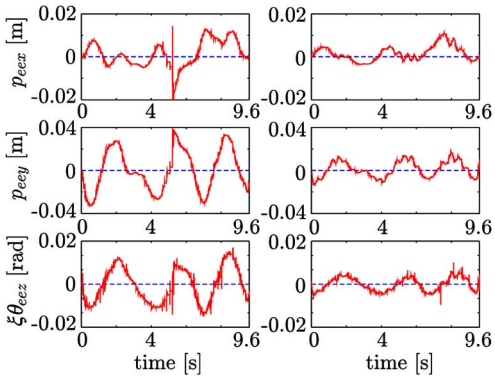

Fig. 16. Estimation error in the target tracking: left side: with Gain A; right side: with Gain B.

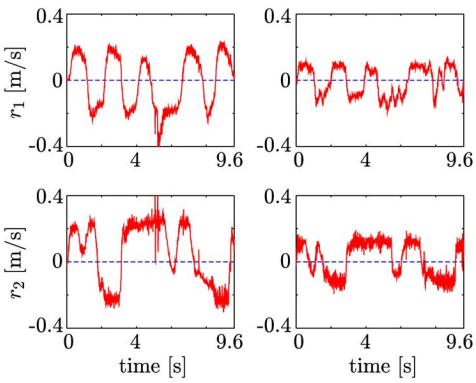

Fig. 17. Velocity error in the target tracking: left side: with Gain A; right side: with Gain B.

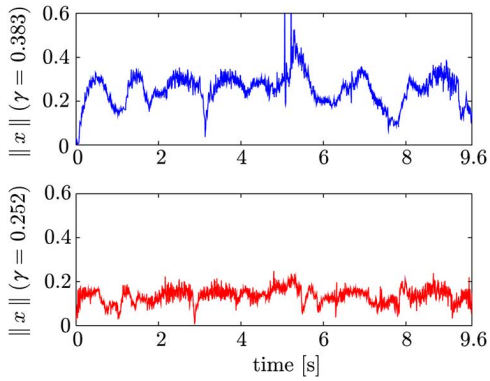

Fig. 18. Norm of the state in the target tracking: top: with Gain A; bottom: with Gain B.

Gain B) $\gamma = 0.252$, $K_c = \mathrm{diag}\{30, 30, 15, 15, 15, 30\}$, $k_e = 20$, $K_r = \mathrm{diag}\{10, 10\}$.

Figs. 15–17 show the control error e_c, the estimation error e_e, and the velocity error r for the target tracking, respectively. The errors in the case of Gain A and B are shown in the left side and the right one of these figures, respectively. In Fig. 18, the top and bottom graph show the norm of the state x in the case of Gain A and B, respectively. The tracking performance is improved for the smaller values of γ from Figs. 15–18. Thus, the experimental results show that L_2-gain is adequate for the performance measure of the dynamic visual feedback control.

Finally, we compare the proposed control law with another one. Since the previous work [17] presents the passivity-based control for the 3-D dynamic visual feedback system which includes the manipulator dynamics, we consider that the comparison between the proposed method and the other one [17] is significant. We design the control parameters such that $K_p = \mathrm{diag}\{6, 1.2, 6, 1.2, 6, 1.2, 6, 1.2\} \times 10^{-4}$ and $K_v = \mathrm{diag}\{20, 40\}$ by the trial and error.

Specifically, we focus on the trajectories of the end-effector and the target object, because the control objective of the visual feedback system is to track the moving target object in a 3-D workspace by image information. In Figs. 19–21, the solid line and the dashed line are the trajectories of the tip of the end-effector and the target object, respectively. Figs. 19 and 20 show the translation along the x and y axes, respectively. Fig. 21 depicts the rotation along the z-axis. The case of our

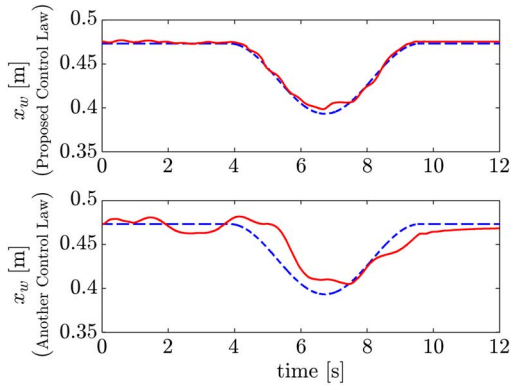

Fig. 19. Trajectories of the translation along the x-axis: top: with proposed control law; bottom: with another one.

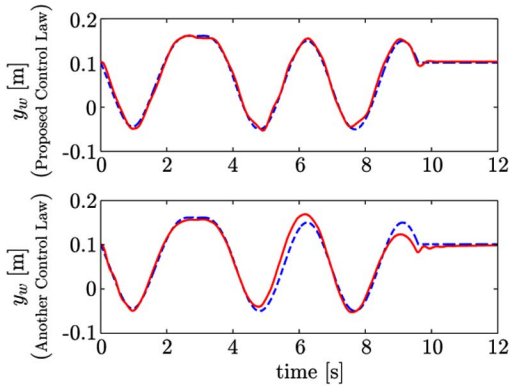

Fig. 20. Trajectories of the translation along the y-axis: top: with proposed control law; bottom: with another one.

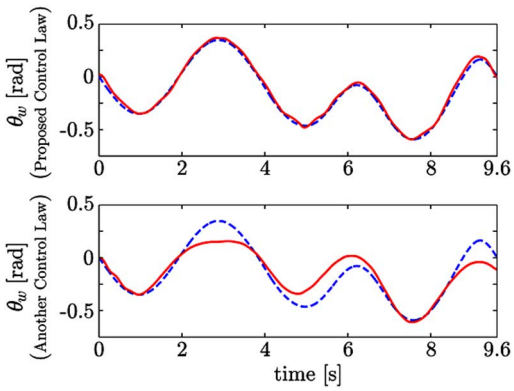

Fig. 21. Trajectories of the rotation along the z-axis: top: with proposed control law; bottom: with another one.

proposed method and the other one [17] are in the top graphs and the bottom ones of Figs. 19–21, respectively. Both methods can achieve the control objective, i.e., tracking for the moving target object. The merits of the method in [17] is that the control law can be simply designed and implemented. Although our proposed method is not as simple to design and implement, the advantage is that the tracking performance in a 3-D workspace is better as depicted in Figs. 19–21. Hence, we consider that the difference in the definition of the error, i.e., defined in the image plane or in a Cartesian space, affects the behavior of the end-effector.

VIII. Conclusions

This paper investigates the dynamic visual feedback control for 3-D target tracking. The main contribution of this paper is to show that the dynamic visual feedback system preserves the passivity of the visual feedback system. A passivity-based observer is designed to estimate the rigid body motion from visual measurements. Stability and L_2-gain performance analysis for the dynamic visual feedback system are discussed based on passivity and dissipative systems theory. Finally, experiment results are presented to verify the stability and L_2-gain performance of the dynamic visual feedback system. Future problems to be addressed using this approach include the questions of global stability, visibility, and so on.

References

[1] S. Hutchinson, G. D. Hager, and P. I. Corke, "A tutorial on visual servo control," *IEEE Trans. Robot. Autom.*, vol. 12, no. 5, pp. 651–670, Oct. 1996.

[2] H. I. Christensen and P. Corke, "Editorial: Special issue on visual servoing," *Int. J. Robot. Res.*, vol. 22, no. 10–11, pp. 779–780, 2003.

[3] S. Yu and B. J. Nelson, "Autonomous injection of biological cells using visual servoing," in *Experimental Robotics VII*. New York: Springer-Verlag, 2001, pp. 169–178.

[4] K. Omote *et al.*, "Self-guided robotic camera control for laparoscopic surgery compared with human camera control," *Amer. J. Surgery*, vol. 177, no. 4, pp. 321–324, 1999.

[5] N. P. Papanikolopoulos, P. K. Khosla, and T. Kanade, "Visual tracking of a moving target by a camera mounted on a robot: A combination of control and vision," *IEEE Trans. Robot. Autom.*, vol. 9, no. 1, pp. 14–35, Feb. 1993.

[6] A. Kawabata and M. Fujita, "Design of an H_∞ filter-based robust visual servoing system," *Contr. Eng. Practice*, vol. 6, no. 2, pp. 219–225, 1998.

[7] F. Chaumette, "Potential problems of stability and convergence in image-based and position-based visual servoing," in *The Confluence of Vision and Control*. New York: Springer-Verlag, 1998, pp. 66–78.

[8] C.-P. Lu, G. D. Hager, and E. Mjolsness, "Fast and globally convergent pose estimation from video images," *IEEE Trans. Pattern Anal. Mach. Intell.*, vol. 22, no. 6, pp. 610–622, 2000.

[9] E. Malis, F. Chaumette, and S. Boudet, "2-1/2-D visual servoing," *IEEE Trans. Robot. Autom.*, vol. 15, no. 2, pp. 238–250, 1999.

[10] P. I. Corke and S. A. Hutchinson, "A new partitioned approach to image-based visual servo control," *IEEE Trans. Robot. Autom.*, vol. 17, no. 4, pp. 507–515, Aug. 2001.

[11] G. Chesi, K. Hashimoto, D. Prattichizzo, and A. Vicino, "Keeping features in the field of view in eye-in-hand visual servoing: A switching approach," *IEEE Trans. Robot.*, vol. 20, no. 5, pp. 908–913, Oct. 2004.

[12] R. Kelly, "Robust asymptotically stable visual servoing of planar robots," *IEEE Trans. Robot. Autom.*, vol. 12, no. 5, pp. 759–766, Oct. 1996.

[13] A. Maruyama and M. Fujita, "Robust control for planar manipulators with image feature parameter potential," *Adv. Robot.*, vol. 12, no. 1, pp. 67–80, 1998.

[14] ——, "Adaptive H_∞ control for robust visual feedback system," in *Proc. 37th IEEE Conf. Dec. Contr.*, 1998, pp. 2283–2288.

[15] B. E. Bishop and M. W. Spong, "Adaptive calibration and control of 2D monocular visual servo systems," *Contr. Eng. Practice*, vol. 7, no. 3, pp. 423–430, 1999.

[16] E. Zergeroglu, D. M. Dawson, M. S. de Queiroz, and A. Behal, "Vision-based nonlinear tracking controllers with uncertain robot-camera parameters," *IEEE/ASME Trans. Mechatron.*, vol. 6, no. 3, pp. 322–337, Sep. 2001.

[17] R. Kelly, R. Carelli, O. Nasisi, B. Kuchen, and F. Reyes, "Stable visual servoing of camera-in-hand robotic systems," *IEEE Trans. Mechatron.*, vol. 5, no. 1, pp. 39–48, Mar. 2000.

[18] N. J. Cowan, J. D. Weingarten, and D. E. Koditschek, "Visual servoing via navigation functions," *IEEE Trans. Robot. Autom.*, vol. 18, no. 4, pp. 521–533, Aug. 2002.

[19] A. Maruyama and M. Fujita, "Visual feedback control of rigid body motion based on dissipation theoretical approach," in *Proc. 38th IEEE Conf. Dec. Contr.*, 1999, pp. 4161–4166.

[20] M. Fujita, A. Maruyama, and H. Kawai, "Observer based dynamic visual feedback control for nonlinear robotics systems," in *Proc. 15th IFAC World Congr. Automat. Contr.*, 2002, pp. 1637–1637.
[21] R. Murray, Z. Li, and S. S. Sastry, *A Mathematical Introduction to Robotic Manipulation*. Boca Raton, FL: CRC, 1994.
[22] F. Bullo and R. Murray, "Tracking for fully actuated mechanical systems: A geometric framework," *Automatica*, vol. 35, no. 1, pp. 17–34, 1999.
[23] A. van der Schaft, *L_2-Gain and Passivity Techniques in Nonlinear Control*, 2nd ed. New York: Springer-Verlag, 2000.
[24] H. Michel and P. Rives, "Singularities in the determination of the situation of a robot effector from the perspective view of 3 points," INRIA, Le Chesnay Cedex, France, 1993.
[25] M. W. Spong and M. Vidyasagar, *Robot Dynamics and Control*. New York: Wiley, 1989.
[26] H. Berghuis and H. Nijmeijer, "A passivity approach to controller-observer design for robots," *IEEE Trans. Robot. Autom.*, vol. 9, no. 6, pp. 740–754, Sep. 1993.
[27] M. Takegaki and S. Arimoto, "A new feedback method for dynamic control of manipulators," *Trans. ASME, J. Dyn. Syst., Meas., Contr.*, vol. 103, no. 2, pp. 119–125, 1981.
[28] R. Ortega and M. W. Spong, "Adaptive motion control of rigid robots: A tutorial," *Automatica*, vol. 25, no. 6, pp. 877–888, 1989.
[29] M. W. Spong, "On the robust control of robot manipulators," *IEEE Trans. Autom. Contr.*, vol. 37, no. 11, pp. 1782–1786, Nov. 1992.
[30] S. Arimoto and T. Nakayama, "Another language for describing motions of mechatronics systems: A nonlinear position-dependent circuit theory," *IEEE/ASME Trans. Mechatron.*, vol. 1, no. 2, pp. 168–180, Jun. 1996.
[31] J. M. A. Scherpen and R. Ortega, "On nonlinear control of euler-lagrange systems: Disturbance attenuation properties," *Syst. Contr. Lett.*, vol. 30, no. 1, pp. 49–56, 1997.
[32] S. Battilotti and L. Lanari, "Adaptive disturbance attenuation with global stability for rigid and elastic joint robots," *Automatica*, vol. 33, no. 2, pp. 239–243, 1997.
[33] K. Zhou and J. C. Doyle, *Essentials of Robust Control*. Englewood Cliffs, NJ: Prentice-Hall, 1998.

Masayuki Fujita (M'88) received the B.E., M.E., and Dr. Eng. degrees in electrical engineering from Waseda University, Tokyo, Japan, in 1982, 1984, and 1987, respectively.

From 1985 until 1992, he was with the Department of Electrical and Computer Engineering, Kanazawa University, Kanazawa, Japan. He was on the faculty of the Japan Advanced Institute of Science and Technology, Ishikawa, Japan, as an Associate Professor from 1992 to 1998, and Kanazawa University as a Professor in 1999. From 1994 to 1995, he held a visiting position in the Department of Automatic Control Engineering, Technical University of Munich, Germany. Since 2005, he has been a Professor of the Department of Mechanical and Control Engineering at Tokyo Institute of Technology, Tokyo, Japan. His research interests include robust control and its applications and passivity-based visual feedback. He is currently an Associate Editor of the IEEE TRANSACTIONS ON AUTOMATIC CONTROL, *Automatica*, and *Asian Journal of Control.*

Dr. Fujita received the Best Paper Award from the Society of Instrument and Control Engineers (SICE) in 1997, and from the Institute of Systems, Control, and Information Engineers (ISCIE) in 2000.

Hiroyuki Kawai (M'04) received the B.S. degree in electrical and computer engineering from Kanazawa University, Kanazawa, Japan, in 1999, and the M.S. and Ph.D. degrees from the Graduate School of Natural Science and Technology, Kanazawa University, in 2001 and 2004, respectively.

From 2004 until 2005, he was the Postdoctoral Scholar of the Information Technology Research Center, Hosei University, Hosei, Japan. He has been an Assistant Professor at Kanazawa Institute of Technology since Spring 2005. His research interests include the visual feedback control of robot systems and the networked cellular vision system. In particular, he is interested in passivity-based control.

Mark W. Spong (S'81–M'81–SM'89–F'96) received the B.A. degree (*magna cum laude*) in mathematics and physics from Hiram College, Hiram, OH, in 1975, the M.S. degree in mathematics from New Mexico State University, Las Cruces, in 1977, and the M.S. and D.Sc. degrees in systems science and mathematics from Washington University, St. Louis, MO, in 1979 and 1981, respectively.

He has been at the University of Illinois at Urbana-Champaign, Urbana-Champaign, since 1984, and is currently Donald Biggar Willett Professor of Engineering, Professor of Electrical and Computer Engineering, and Research Professor in the Coordinated Science Laboratory. He has published over 200 technical articles in control and robotics and is co-author of three books. In addition, he is President of Mechatronic Systems, Inc., a company that he founded in 1996 to produce and market innovative laboratory experiments for control systems research and education.

Dr. Spong is a member of Phi Beta Kappa. He received the Senior Scientist Research Award from the Alexander von Humboldt Foundation, the Distinguished Member Award from the IEEE Control Systems Society, and the IEEE Third Millennium Medal. Additional honors include the O. Hugo Schuck and John R. Ragazzini awards from the American Automatic Control Council. He is Past-President of the IEEE Control Systems Society. Within the IEEE, he has also served as Vice President for Publication Activities of the Control Systems Society from 2000–2002, Editor-in-Chief of the IEEE TRANSACTIONS ON CONTROL SYSTEMS TECHNOLOGY from 1997–2000, and as an Associate Editor for the IEEE TRANSACTIONS ON AUTOMATIC CONTROL, the IEEE TRANSACTIONS ON CONTROL SYSTEMS TECHNOLOGY, the IEEE TRANSACTIONS ON ROBOTICS AND AUTOMATION, and the *IEEE Control Systems Magazine*. He served on the Board of Governors of the Control Systems Society from 1994–2002.